ChemPubSoc Europe

DOI: 10.1002/cphc.201402532

A Theoretical Study of the Interaction of Hydrogen and Oxygen with Palladium or Gold Adsorbed on Pyridine-Like Nitrogen-Doped Graphene

Eduardo Rangel,*[a, c] Luis Fernando Magana,[b] and Luis Enrique Sansores[a]

The interaction of H_2 and O_2 molecules in the presence of nitrogen-doped graphene decorated with either a palladium or gold atom was investigated by using density functional theory. It was found that two hydrogen molecules were adsorbed on the palladium atom. The interaction of these adsorbed hydrogen molecules with two oxygen molecules generates two hydrogen peroxide molecules first through a Eley–Rideal mechanism and then through a Langmuir–Hinshelwood mechanism. The barrier energies for this reaction were small; therefore, we expect that this process may occur spontaneously at room temperature. In the case of gold, a single hydrogen molecule is adsorbed and dissociated on the metal atom. The interaction of the dissociated hydrogen molecule on the surface with one oxygen molecule generates a water molecule. The competitive adsorption between oxygen and hydrogen molecules slightly favors oxygen adsorption.

1. Introduction

Theoretical and experimental research has recently been focused on the catalytic properties of nitrogen-doped graphene. Nitrogen doping has proved to be an effective way to adjust the properties of graphene and nanotubes and render their potential use for various applications.[1–11] In particular, several studies have approached the problem of hydrogen storage and catalytic reactions on nitrogen-doped graphene decorated with Pd.[2,12–13] The decoration of palladium on nitrogen-doped graphene has been recently achieved and studied by Parambhath and co-workers;[2] they found that a maximum hydrogen capacity of 4.4 wt% can be achieved at 25 °C and 4 MPa. Motivated by these experimental results, we recently studied the interaction of hydrogen molecules with small palladium clusters supported on pyridine-like nitrogen-doped graphene (PNG).[14] Our calculations showed that the support has a significant influence on the electronic properties of palladium clusters and leads to three types of adsorption states for hydrogen.

[a] Dr. E. Rangel, Dr. L. E. Sansores
Dept. Materia condensada y criogenia
Instituto de Investigaciones en Materiales
Universidad Nacional Autónoma de México
Apartado Postal 70-360
C.P. 04510, México, D. F. (Mexico)
E-mail: kovoldedu@yahoo.com.mx

[b] Dr. L. F. Magana
Dept. Estado Sólido, Instituto de Física
Universidad Nacional Autónoma de México
Apartado Postal 20-364
C.P. 01000, México, D. F. (Mexico)

[c] Dr. E. Rangel
Dept. Biotecnología, Escuela Superior de Apan
Universidad Autónoma del Estado de Hidalgo
Carretera Apan-Calpulalpan, Km.8.
Chimalpa Tlalayote s/n, Colonia Chimalpa
Apan, Hgo., México. C.P. 43900 (Mexico)

In relation to catalytic reactions, an alternative route to the conventional technology of the formation of hydrogen peroxide, which avoids the use of anthraquinone,[15] is the direct reaction between molecular hydrogen and oxygen in the presence of a catalyst.[16] Most of the catalysts used for the direct synthesis of H_2O_2 are prepared from palladium or gold supported on a variety of substrates such as alumina, silica, and carbon.[17] However, the use of N-functionalized carbon nanotubes or graphene as a support can lead to an increase in the yield of H_2O_2. We found only one experimental study of the direct synthesis of H_2O_2 on palladium and gold-palladium nanoparticles supported on N-functionalized carbon nanotubes.[18] Arrigo and co-workers studied the nanostructural transformation accompanying the loss of activity and selectivity for hydrogen peroxide synthesis.[18] However, they did not study the possible reactions that could occur on modified N-functionalized carbon.

An ambiguous and complex mechanism is hidden behind the seemingly simple chemical reaction between H_2 and O_2 for H_2O_2, H_2O, OH, and OOH formation. Such reactions can be described by Eley–Rideal[19] or/and Langmuir–Hinshelwood[20] mechanisms. According to the first mechanism, $O_{2(g)}$ from the gas phase reacts directly with adsorbed $H_{(s)}$ or $H_{2(s)}$ forming $OH_{(s)}$ and $OOH_{(s)}$ (s and g indicate that the atom or molecule are either adsorbed or gas phase, respectively), and vice versa, the gas phase $H_{2(g)}$ molecule interacts with adsorbed $O_{2(s)}$. Langmuir–Hinshelwood mechanism implies interaction of co-adsorbed molecules ($O_{2(s)}$, $H_{2(s)}$, $O_{(s)}$, $H_{(s)}$, $OOH_{(s)}$) with each other.

The objective of this work was to study the interaction between H_2 and O_2 in the presence of PNG decorated with a gold or palladium atom. It should be mentioned that several groups have observed three different types of nitrogen in nitrogen-doped graphene (N-graphene) systems; these are pyridinic nitrogen, pyrrolic nitrogen, and the nitrogen atoms of

C–N bonds.[3–5] Pure PNG has recently been synthesized by Luo et al.[21] Here, we did not study pyrrolic-nitrogen-doped graphene or the C–N bond, which will be a matter of further study.

We focused our attention on H_2O_2, H_2O, OH, and OOH formation. Therefore, it is important to understand the possible reactions that can occur on the modified graphene. Nevertheless, competitive processes of adsorption of H_2 and O_2 molecules were also studied.

2. Results and Discussion

The study was carried out in five steps: 1) adsorption of the metal (Au or Pd) onto the PNG, 2) adsorption of H_2 onto the PNG–metal system, 3) adsorption of O_2 onto the PNG–metal–hydrogen system, 4) adsorption of oxygen onto the PNG–metal system, and 5) adsorption of hydrogen molecules onto the PNG–metal–oxygen system.

2.1. Adsorption of the Metal Atom

First, optimization of the PNG layer was performed; as shown in Figure 1 a, the three nitrogen atoms have lone pairs of electrons that form highly localized acceptor-like states (HOMO) at the Fermi level. Nonbonding electrons are localized in an sp^2 orbital, which may form chemical bonds under electrophilic attack. As a consequence, the PNG becomes a π acceptor (LUMO).

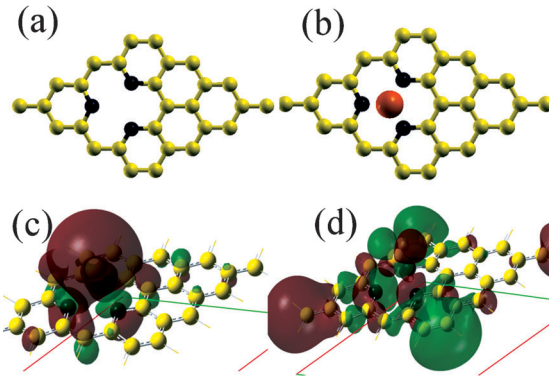

Figure 1. a) Unit cell of the optimized PNG layer. b) Adsorption sites for metal on PNG layer. Position on vacancy is the most stable. c) HOMO and d) HOMO-1 for PNG-Au. The red surface is isovalue positive and the green surface is isovalue negative.

Starting with the optimized PNG layer, a metal atom was added onto the PNG surface and the new system was optimized. For both cases (Pd and Au), the most stable site was above the vacancy (see Figure 1 b). Clearly, N-graphene vacancy favors the adsorption of metals. In fact, one experimental study indicated that the vacancies in graphene act as trapping centers for metal atoms.[22] The calculated values for the adsorption energy of the Pd and Au atoms are 2.46 and 1.02 eV, respectively. Thus, the metal adsorption energy to vacancy is smaller than its cohesive energy (3.90 and 3.25 eV for Pd and Au, respectively), which may result in metal clustering on nitrogen-doped graphene. A strong binding of metal adatoms with the vacancy sites of PNG essentially implies lesser metal adatom migration on the adsorbent surface, which is helpful for formation of smaller clusters rather than large aggregations and is advantageous in practical applications.[14,23] When the metal is absorbed onto the PNG, the metal is bound to the three nitrogen atoms, with small changes in the carbon–nitrogen bond length. When the metal is a gold atom, the average C–N distance increases from 1.329 to 1.349 Å. The C–C–N angle changes from 120.33 to 119.26°, and the C–N–C angle reduces from 123.12 to 123.04°. When the metal is a Pd atom, the C–N distance is 1.346 Å, the C–C–N angle is 119.79°, and the C-N-C angle is 122.85°. The metal–nitrogen average bond lengths are 2.20 and 2.35 Å for Pd and Au, respectively. Löwdin population analysis shows that Pd and Au have a net positive charge $+0.6$ and $+0.07$, respectively. In the case of palladium, nitrogen atoms have a net negative charge of -0.25 atom^{-1}. When metal atoms are bonded to N atoms, electronic charge from Pd is transferred to the N-graphene system. As a consequence, electronic charge fills acceptor-like states. In the case of gold, we found that the attachment of a gold atom onto the pyridinic support occurs by a small donation of electrons from Pd 6s and 6p orbitals to C 2s and N p orbitals and then a back-donation from N p to Pd 5d orbitals.

An orbital analysis was performed to find additional information of chemical bonding. As examples, spin configuration and magnetic moment were determined as a contribution of the most localized nonbonding d-orbitals. An orbital analysis of the Au–PNG system shows that the HOMO is a bonding orbital with contributions from the metal s orbital and carbon p orbitals (Figure 1 c). HOMO-1 is a bonding orbital with contributions from N $2p_z$ and Pd $4d_z^2$ orbitals (Figure 1 d). In contrast, for the Pd–PNG system the HOMO is a nonbonding d-orbital and HOMO-1 is a bonding orbital with contributions from N $2p_z$ and Pd $4d_z^2$ orbitals. As a consequence, the Au–PNG does not have a magnetic moment, whereas the magnetic moment of every atom in the Pd–PNG system was calculated and it was found that the magnetic moment of Pd atom is 0.67 μ_B and 0.18, 0.08 and 0.097 μ_B for N1, N2 and N3, respectively. For HOMO and HOMO-1 orbitals shown in Figure 1 c an 1 d, the red surface is isovalue positive and the green surface is isovalue negative.

2.2. H_2 Interaction with Metal–PNG

The interaction of metal–PNG systems with H_2 was studied to explore their capacity to adsorb hydrogen molecules. The first H_2 molecule was initially located on top of the Pd or Au atoms, then the system was optimized. For the Pd–PNG system, a second H_2 molecule was located around Pd atom and optimized. Initially this molecule was far from previous H atoms. However, among the many different configurations tried for H_2 adsorption, we found that the initial orientation of the molecules of H_2 onto the metal atoms had no influence on the result.

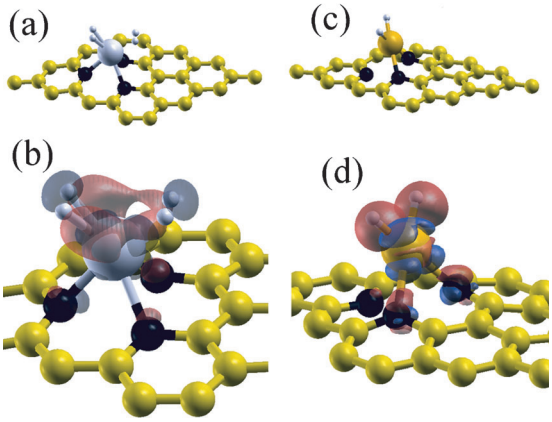

Figure 2. a) Adsorption of two hydrogen molecules around the Pd atom anchored on the PNG vacancy. b) Adsorption and dissociation of a single hydrogen molecule around the Au atom. Surfaces of constant electron-density difference for c) PNG–Pd–$2H_2$ and d) PNG–Au–2H, respectively. The two isosurfaces correspond to values of $\Delta\rho(r) = \pm 5.0\times10^{-2}$ e a.u.$^{-3}$. The red and blue surfaces are isovalues positive and negative, respectively.

The optimized system showed that the Pd atom anchored on the PNG can bind up to two hydrogen molecules (Figure 2a). The adsorption energy for the first H_2 molecule is 1.2 eV, with Pd–H average distance 1.76 Å and H–H bond distance 0.87 Å. For the second molecule, the adsorption energy is 0.90 eV, with average Pd–H distance 1.88 Å and H–H bond distance of 0.81 Å. Ultimately, the C–N bonds remained unchanged and the metal–N bond lengthened slightly, indicating that the Pd–N interaction is reduced.

On H_2 adsorption, a certain number of electrons are transferred from occupied metal d orbitals to the antibonding (σ^*) state of H_2, a process known as back donation (also as Kubas-type binding[24]). However, the unoccupied Pd d orbitals are related to the long-range interaction with the (σ) bonding state of H_2 and determine the number of adsorbed H_2. Nudged elastic band (NEB) calculations show that molecular activation occurs without a barrier.

The donation and back donation are shown for the Pd case in Figure 2b. We have plotted two surfaces of constant electron-density difference. The two isosurfaces correspond to values of $\Delta\rho(r) = \pm 5.0\times10^{-2}$ e a.u.$^{-3}$ ($\Delta\rho = \rho(\text{PNG+metal}+n\text{H}_2) - \rho(\text{PNG+metal}) - \rho(n\text{H}_2)$). The red surface with positive $\Delta\rho$ is the region in which electronic charge concentrates after interacting between hydrogen molecules and palladium atom. On the other hand, the blue region, with negative $\Delta\rho$, is the region in which electronic charge is lost after the interaction between hydrogen molecules and metal atom.

In the case of gold, a single hydrogen molecule is adsorbed and dissociated on the metal atom (Figure 2c). Adding the second hydrogen molecule, as for Pd, does not give a bonded state. The adsorption energy is 2.33 eV H_2^{-1}. The average distance Au–H is 1.57 Å and the H–H bond distance is 1.95 Å. The C–N bonds remained unchanged and the metal–N bond is lengthened slightly. The donation of electronic charge from the Pd atom to the dissociated H_2 molecule is shown in Figure 2d. The two isosurfaces correspond to values of $\Delta\rho(r) = \pm 5.0\times10^{-2}$ e a.u.$^{-3}$ ($\Delta\rho = \rho(\text{PNG+metal}+n\text{H}_2) - \rho(\text{PNG+metal}) - \rho(n\text{H}_2)$). The red surface with positive $\Delta\rho$ is the region in which electronic charge concentrates after interacting with a single hydrogen molecule and a gold atom. Notably, in both cases, electrons are transferred to the hydrogen atoms. NEB shows molecular dissociation occurs without a barrier.

2.3. O_2 Interaction with PNG–Metal Hydrogenated System

Two oxygen molecules are then added to the system. Optimization was performed by adding first one molecule then optimized again after adding the second molecule. The direct interaction of the two adsorbed hydrogen molecules, with two oxygen molecules generates two hydrogen peroxide molecules around the palladium atom.

We employed the NEB method to determine the reaction path shown in Figure 3a, when one O_2 was added, and Figure 3b when the second molecule was added to the H_2–Pd–PNG system. The activation energies were small, 0.129 and 0.202 eV for the formation of the first and second hydrogen peroxide molecules, respectively. In Figure 3a, we show the initial, final, and three transition states. These steps show the initial state (Step 1), the interaction of O_2 molecule with the $2H_{2(S)}$ (Step 2), formation of the first $OOH_{(s)}$ (Step 3), interaction of

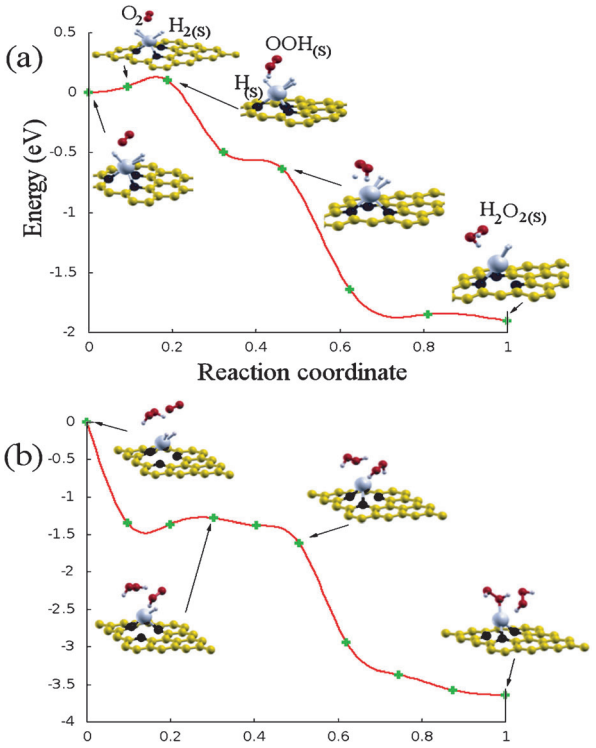

Figure 3. Energy path along the reaction coordinate obtained with the NEB method for the formation of the first hydrogen peroxide molecule. The steps show the initial state (Step 1), the interaction of O_2 molecule with the $2H_{2(S)}$ (Step 2), formation of the first $OOH_{(S)}$ (Step 3), interaction of $OOH_{(S)}$ with $H_{(s)}$ (Step 5), and generation of $H_2O_{2(s)}$ molecule around the palladium atom (Step 8). b) After a second oxygen molecule interacts with the system, another hydrogen peroxide molecule is formed.

the $OOH_{(s)}$ with $H_{(s)}$ (Step 5), and generation of $H_2O_{2(s)}$ molecule around the palladium atom (Step 8). The smallest Pd–O bond distance is 2.15 Å, and the O–O bond distance is 1.49 Å. Steps 1–3 are described by Eley–Rideal mechanisms. The O_2 molecule from the gas phase reacts directly with $H_{2(S)}$, forming $OOH_{(S)}$. Steps 4–7 are described by the Langmuir–Hinshelwood mechanisms; this implies that co-adsorbed molecules $OOH_{(s)}$ interact with other ($H_{(s)}$) forming $H_2O_{2(s)}$.

When a second oxygen molecule was added, it interacted with the system and another hydrogen peroxide molecule was formed (Figure 3 b); the process can be described by Eley–Rideal followed by Langmuir–Hinshelwood mechanisms. The O–O bond distance for the second H_2O_2 molecule was 1.47 Å, the corresponding shortest Pd–O distance was 2.032 Å. For the whole process, initially a very small energy barrier of 0.129 eV was found. After this barrier was overcome, sufficient energy was available for the process to continue. A negative value of the changes of Gibbs energy and low activation energies in Step 3 (Figure 3 a), and Step 4 (Figure 3 b) favor the formation of $H_2O_{2(s)}$. This means that the process might occur spontaneously at room temperature. To study the desorption process, molecular dynamics calculations at atmospheric pressure were performed. We considered temperatures of 300, 500, and 900 K, and a time step of one femtosecond, with the Andersen thermostat method.[25] At approximately 900 K, and after 0.5 ps, hydrogen peroxide $H_2O_{2(g)}$ molecules are desorbed. Whereas a 0.5 ps time MD simulation is already computationally quite costly, it is not long enough to observe desorption at lower temperatures. However, it does suggest that the system is quite stable and that it is possible to extract the H_2O_2 molecules without breaking the Pd–N bond.

In the case of gold, the direct interaction of the two adsorbed hydrogen atoms with one oxygen molecule generates two OH molecules that are weakly bonded between them (Figure 4). The activation energy is 0.401 eV. The initial, final and two transition states are shown in Figure 4. These steps show the initial state (Step 1), the interaction of O_2 molecule with one $H_{(s)}$ (Step 3), formation of the first $OOH_{(s)}$ (Step 5), and generation of two $OH_{(s)}$ molecule around the gold atom (Step 8). The corresponding shortest Au–OH distance is 2.0 Å, and the O–O bond distance is 1.98 Å. The presence of the oxygen molecules does not change the C–N distances in the PNG whereas the metal–N bonds are slightly shortened in the case of Pd and increased in the case of Au. Once again, the steps are described by the Eley–Rideal mechanism followed by the Langmuir–Hinshelwood mechanism. To study the desorption process, we considered temperatures from 300 and 500 K, and a time step of one femtosecond. The first important change occurs at 300 K. We observe a fast decrease in energy. This corresponds to OH–OH dissociation to form a water molecule. The water molecule is desorbed and the other oxygen atom stays bonded to the gold atom. It is clear that the formation of H_2O requires breaking of the O–O bond in at least one of the intermediates ($O_{2(s)}$, $OOH_{(s)}$, and $H_2O_{2(s)}$). Once the O–O bond is broken on a surface, it cannot be formed again.

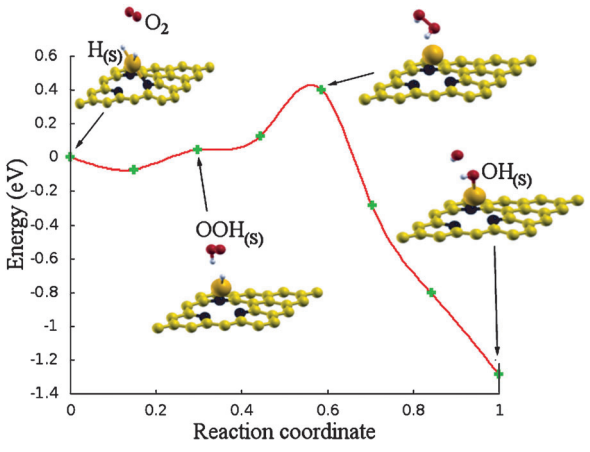

Figure 4. a) Energy path along the reaction coordinate obtained with the NEB method for the formation of the OH molecules. The steps show the initial state, the interaction of O_2 molecule with the $2H_{(s)}$ (Step 1), formation of the first $OOH_{(s)}$ (Step 3), interaction of $OOH_{(s)}$ with $H_{(s)}$ (Step 5), and generation of $OH_{(s)}$ molecules around the gold atom.

2.4. H_2 Interaction with Pd–O_2–PNG and Au–O_2–PNG

According to the previous discussion, the interaction of O_2 with metal–PNG hydrogenated systems was studied. We found that an O_2 molecule from the gas phase reacts directly with $H_{2(s)}$, forming $OOH_{(s)}$. According to most quantum chemical data, OOH hydrogenation is the rate-determining step in H_2O_2 synthesis[26–29] so that $OOH_{(s)}$ is the main precursor. Hence, the other reaction path is the interaction between H_2 and metal–PNG oxidized system, to obtain a molecule of hydrogen peroxide.

First, the interaction of an O_2 molecule with the Pd–PNG and Au–PNG systems were analyzed (Step 1 in Figure 5 a and Step 1 in Figure 5 b). In the optimized system, the metal atom (Pd or Au) anchored on the PNG can bind only one O_2 molecule. The adsorption energy was 2.57 eV for Pd and 2.06 eV for Au. The average Pd–O bond distance was 2.05 Å and the average Au–O distance was 2.04 Å. The O–O bond distance around Pd and Au was 1.35 and 1.4 Å, respectively. Afterwards, the interaction of one hydrogen molecule with the newly formed system was studied, as shown in Figure 5 (a and b) for Pd and Au, respectively.

The reaction coordinate, which presents a large activation energy (1.22 eV) and positive change in Gibbs energy is shown in Figure 5 a. This means that the process followed to obtain a molecule of hydrogen peroxide cannot occur spontaneously. Nevertheless, the inverse process to obtain one molecule of $H_{2(g)}$ in the gas phase and one molecule of $O_{2(s)}$ from $H_2O_{2(s)}$ could occur, with the energy barrier being 0.9 eV. According to the "absolute rate theory" this reaction should present slow kinetics, and require high temperatures to take place. Therefore, the readsorption of $H_2O_{2(s)}$ and $H_2O_{2(g)}$ does not lead to any decomposition in others molecules (OH, H_2O, and OOH) at moderate temperature.

On the other hand, in the case of gold, direct interaction of one molecule of $H_{2(g)}$ in the gas phase with one molecule of $O_{2(s)}$ adsorbed on a Au atom, generates one water molecule $H_2O_{(s)}$, and the second oxygen atom remains bonded to the

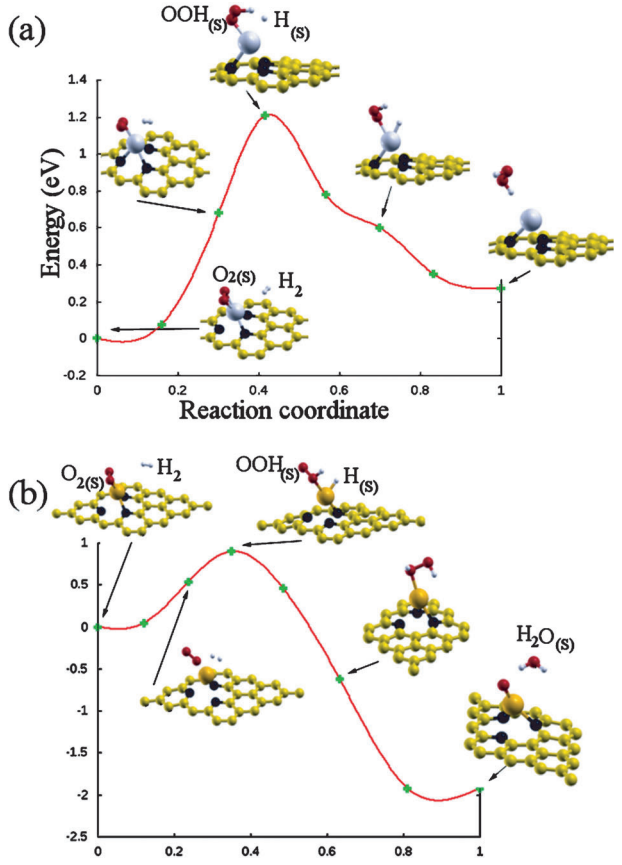

Figure 5. a) Energy path along the reaction coordinate obtained with the NEB method for the formation of the hydrogen peroxide molecule. The steps show the initial state (Step 1), the interaction of H_2 molecule with the $O_{2(s)}$ (Step 3), formation of the first $OOH_{(s)}$ (Step 4), interaction of the $OOH_{(s)}$ with $H_{(s)}$ (Step 6), and generation of $H_2O_{2(s)}$ molecule around the palladium atom (Step 8). b) The steps show the initial state, the interaction of H_2 molecule with the $O_{2(s)}$ (Step 3), formation of the first $OOH_{(s)}$ (Step 4), interaction of $OOH_{(s)}$ with $H_{(s)}$ (Step 6), and formation of $H_2O_{(s)}$ molecule around the gold atom.

gold atom (Figure 5 b). Once again, the steps are described by the Eley–Rideal mechanism followed by the Langmuir–Hinshelwood mechanism. The initial, final, one transition state and two intermediates are shown in Figure 5 b. These steps show the interaction of H_2 molecule with the $O_{2(s)}$ (Step 3), formation of the first $OOH_{(s)}$ (Step 4), and generation of a water molecule $H_2O_{(s)}$ (Step 8). The corresponding average Au–H bond distance is 2.0 Å. The barrier energy is 0.8 eV. This reaction should present slow kinetics and require high temperatures to occur.

2.5. Competition between Hydrogen and Oxygen Molecules

In the last two sections, we studied the reaction paths for the interaction between $O_{2(g)}$ and metal–PNG hydrogenated system and the interaction between $H_{2(g)}$ and metal–PNG oxidized system, respectively. However, H_2 and O_2 molecules may both be present in the gas phase. It is possible that they compete for adsorption onto the Pd or Au. To study this competition, we calculated the oxygen displacement energy that corresponds to the energy required to replace the adsorbed $O_{2(S)}$ by n $H_{2(S)}$ adsorbed hydrogen molecules. In the case of Pd, the results for E_d considering different number of hydrogen molecules are: for one H_2, E_d was 1.74 eV, for two H_2 molecules, E_d was 0.50 eV. It is found that, in the first case, replacement of $O_{2(s)}$ by $H_{2(s)}$ is energetically impeded. In the second case, replacement of $O_{2(s)}$ by $2H_{2(s)}$ is energetically possible. For Au, the energy required to replace the adsorbed $O_{2(s)}$ by $H_{2(s)}$ adsorbed and dissociated is 0.166 eV. It is shown that the competitive adsorption between oxygen and hydrogen molecules slightly favors oxygen for both systems (Pd and Au), respectively. However, the replacement of $O_{2(s)}$ by $H_{2(s)}$ is energetically possible and this fact could be used to favor the formation of hydrogen peroxide in the system decorated with a Pd atom.

3. Conclusions

The interaction of H_2 and O_2 molecules in the presence of nitrogen-doped graphene decorated with a palladium or gold atom was investigated by using density functional theory. First, we optimized the geometry for a metal atom (palladium or gold) adsorbed on PNG. The most stable site in both cases was above the vacancy. We then found that two hydrogen molecules (activated states) adsorbed around an anchored palladium atom. When the hydrogenated system interacted with two oxygen molecules in the gas phase, two hydrogen peroxide molecules formed around the metal atom; this took place through the Eley–Rideal mechanism followed by the Langmuir–Hinshelwood mechanism. We found that the barrier energies for this reaction are small, that is, 0.129 and 0.202 eV for the first and second hydrogen peroxide molecules, respectively. Therefore, we expect this process to occur spontaneously at room temperature. Furthermore, we show that readsorption of the hydrogen peroxide molecule does not lead to any decomposition (OH, H_2O, and OOH) at moderate temperature. In the case of gold, a single hydrogen molecule is adsorbed and dissociated on the metal atom. The interaction of the dissociated hydrogen molecule with one oxygen molecule generates a water molecule. Once again, the steps were described by the Eley–Rideal mechanism followed by the Langmuir–Hinshelwood mechanism. In contrast, the interaction of metal (Pd or Au) adsorbed onto nitrogen-doped graphene with the oxygen molecule before hydrogen molecule, leads to palladium oxidation, with consequent reduction of the adsorption capacity. This means that the competitive adsorption between oxygen and hydrogen molecules slightly favors oxygen for both systems (Pd and Au). However, the replacement of O_2 by H_2 is energetically possible and this fact could be used to favor the formation of hydrogen peroxide in the system decorated with a Pd atom.

Computational Methods

Calculations were done by using density functional theory (DFT) within the general gradient approximation GGA[30] and molecular dynamics (MD)[31,32] with time step of one femtosecond, with the Andersen thermostat[20] method within the Born–Oppenheimer approximation of the Quantum Espresso code.[33] Perdew–Burke–En-

zelhof expression[34] for exchange-correlation energies and norm-conserving Troullier–Martins pseudo potentials,[35] in the fully separable form of Kleinman–Bylander[36] was used. The valence electronic states considered were: for hydrogen 1s, for carbon $2s^2 2p^2$, for oxygen $2s^2 2p^4$, for gold $5d^{9.50} 6s^1 6p^{0.5}$,for palladium $4d^9 5s^1$, and for nitrogen $2s^2 2p^3$.

Nonrelativistic, spin-polarized calculations were performed for both Au and Pd systems. The cut-off energy was set at 1360 eV, and 34 k points within the Monkhorst–Pack special k point scheme[37] was used. The threshold energy convergence was 10^{-6} eV. We undertook the study of the minimum energy path (MEP) for the different reactions by using the nudged elastic band (NEB) method, and the conjugate gradient technique[33] to find the local minima.

The pseudopotentials were validated by performing the following calculations. By energy minimization, the length of the hydrogen molecule bond was calculated to be 0.751 Å. The corresponding experimental value is 0.742 Å.[38] In the same manner, for the hydrogen peroxide molecule, we obtained the following values: H–O bond length: 0.982 Å and H-O-O angle: 101.6°. The experimental values are 0.965 Å and 99.4°, respectively. These data are for hydrogen peroxide molecule with the open book symmetry, which is the most stable.[39,40] In the same way, the calculated lattice parameter of bulk Au was 4.18 Å (the experimental value is 4.08 Å[41]) with a cohesive energy (the difference between the total energy of a solid and the free atoms) of 3.25 eV (the experimental value is 3.81[41]). For palladium, we calculated a lattice parameter of 3.98 Å and cohesive energy 3.90 eV (the experimental values are 3.89 Å and 3.89 eV, respectively[41]); using the same approach, we obtained a value of 1.419 Å for the carbon bond length in graphene (the experimental[38] value is 1.415 Å). To analyze the orbitals and energy gap between the HOMO and LUMO, Gaussian quantum chemistry code with periodic boundary conditions in *x*, *y* was used.[42] Within this code, we used effective LANL2DZ core potentials and a numerical basis set for Au and Pd. For C, N, O and H atoms the basis set (6-31G) was employed.[42] These basis sets were validated with the lattice parameter of graphene. We obtained a value of 1.418 Å for the carbon bond length in graphene (the experimental value is 1.415 Å).

To study the interaction of the metal atom (Au or Pd) with a graphene vacancy, we considered one vacancy per 28 carbon atoms, three nitrogen atoms, and one metal atom (Au or Pd). The system was represented within a hexagonal unit cell with $a = b = 9.75$ Å and $c = 20$ Å and periodic conditions. The magnitude of c was large enough to avoid undesired interactions between adjacent layers along this direction.

The adsorption energy E_b of the metal atom (Au or Pd) on the vacancy was calculated by Equation (1):

$$E_b = [E(\mathrm{PNG} + \mathrm{metal})] - [E(\mathrm{PNG}) + E(\mathrm{metal})] \quad (1)$$

where [E(PNG+metal)] is the total energy of the final optimized configuration and E(PNG) + E(metal) is the total energy of the initial system plus the total energy of gold or palladium atom alone with no interaction between them.

The adsorption energy E_{ad} of hydrogen molecules was obtained from Equation (2):

$$E_{ad} = [E(\mathrm{PNG} + \mathrm{metal} + n\mathrm{H_2})] - [E(\mathrm{PNG} + \mathrm{metal}) + E(n\mathrm{H_2})] \quad (2)$$

where n is the number of hydrogen molecules, E[(PNG+metal+nH$_2$)] is the total energy of the final optimized configuration, and E(PNG+metal) + E (nH$_2$) is the total energy of the initial system, which is the metal (Au or Pd) doped N-graphene alone plus the energy of n hydrogen molecules alone with no interaction between them.

We calculated the oxygen displacement energy that corresponds to the energy required to replace the adsorbed oxygen molecule O_2 by n H_2 adsorbed hydrogen molecules. This displacement energy E_d was calculated by Equation (3):

$$E_d = E(\mathrm{PNG} + \mathrm{metal} + n\mathrm{H_2}) + E(\mathrm{O_2}) - [E(\mathrm{PNG} + \mathrm{metal} + \mathrm{O_2}) + n\mathrm{E}(\mathrm{H_2})] \quad (3)$$

Acknowledgements

We thank Dirección General de Asuntos del Personal Académico for financial support (project IN106514 and E.R.'s scholarship), and DGTIC UNAM for the Supercomputing facilities and technical assistance.

Keywords: adsorption · density functional calculations · graphene · gold · palladium

[1] Z. M. Ao, F. M. Peeters, *J. Phys. Chem. C* **2010**, *114*, 14503 – 14509.
[2] V. B. Parambhath, R. Nagar, S. Ramaprabhu, *Langmuir* **2012**, *28*, 7826 – 7833.
[3] H. Gao, L. Song, W. Guo, L. Huang, D. Yang, F. Wang, Y. Zuo, X. Fan, Z. Liu, W. Gao, R. Vajtai, K. Hackenberg, P. M. Ajayan, *Carbon* **2012**, *50*, 4476 – 4482.
[4] H. Wang, T. Maiyalagan, X. Wang, *ACS Catal.* **2012**, *2*, 781 – 794.
[5] Y. Shao, S. Zhang, M. H. Engelhard, G. Li, G. Shao, Y. Wang, J. Liu, I. A. Aksay, Y. Lin, *J. Mater. Chem.* **2010**, *20*, 7491 – 7496.
[6] http://pubs.acs.org/action/doSearch?ContribStored=Qu%2C+L, http://pubs.acs.org/action/doSearch?ContribStored=Liu%2C+Y, http://pubs.acs.org/action/doSearch?ContribStored=Baek%2C+J, http://pubs.acs.org/action/doSearch?ContribStored=Dai%2C+L. *ACS Nano* **2010**, *4*, 1321 – 1326.
[7] D. Deng, X. Pan, L. Yu, Y. Cui, Y. Jiang, J. Qi, *Chem. Mater.* **2011**, *23*, 1188 – 1193.
[8] D. Usachov, O. Vilkov, A. Grüneis, D. Haberer, A. Fedorov, V. K. Adamchuk, A. B. Preobrajenski, P. Dudin, A. Barinov, M. Oehzelt, C. Laubschat, D. V. Vyalikh, *Nanolett.* **2011**, *11*, 5401 – 5407.
[9] D. Sen, R. Thapa, K. K. Chattopadhyay, *ChemPhysChem* **2014**, *15*, 2542 – 2549.
[10] D. W. Boukhvalov, Y. W. Son, R. S. Ruoff, *ACS Catal.* **2014**, *4*, 2016 – 2021.
[11] S. H. Noh, D. H. Kwak, M. H. Seo, T. Ohsaka, B. Han, *Electrochim. Acta*, **2014**, *140*, 225 – 231.
[12] L. Ma, J. M. Zhang, K. W. Xu, *Appl. Surf. Sci.* **2014**, *292*, 921 – 927.
[13] X. K. Kong, Q. W. Chen, Z. Y. Lun, *ChemPhysChem* **2014**, *15*, 344 – 350.
[14] E. Rangel, E. Sansores, *Int. J. Hydrogen Energ.* **2014**, *39*, 6558 – 6566.
[15] J. M. Campos-Martin, G. Blanco-Brieva, J. L. Fierro, *Angew. Chem. Int. Ed. Angew Chem. Int. Ed.* **2006**, *45*, 6962 – 6984.
[16] E. Rangel, L. F. Magana, L. E. Sansores, G. J. Vázquez, *Mater. Res. Soc. Symp. Proc.* **2012**, *1451*, 69 – 74.
[17] S. Chinta, J. H. Lunsford, *J. Catal.* **2004**, *225*, 249 – 255.
[18] R. Arrigo, M. E. Schuster, S. Abate, S. Wrabetz, K. Amakawa, D. Teschner, M. Freni, G. Centi, S. Perathoner, M. Hävecker, R. Schlögl, *ChemSusChem* **2014**, *7*, 179 – 194.
[19] D. D. Eley, E. K. Rideal, *Nature* **1940**, *146*, 401 – 402.
[20] I. Langmuir, *Trans. Faraday Soc.* **1922**, *17*, 621 – 654.
[21] Z. Luo, S. Lim, Z. Tian, J. Shang, L. Lai, B. MacDonald, *J. Mater. Chem.* **2011**, *21*, 8038 – 8044
[22] J. A. Rodríguez-Manzo, O. Cretu, F. Banhart, *ACS Nano* **2010**, *4*, 3422 – 3428.

[23] D. Sen, R. Thapa, K. K. Chattopadhyay, *Int. J. Hydrogen Energ.* **2013**, *38*, 3041 – 3049.
[24] G. J. Kubas, *Acc. Chem. Res.* **1988**, *21*, 120 – 128.
[25] H. C. Andersen, *J. Chem. Phys.* **1980**, *72*, 2384 – 2393.
[26] D. G. Barton, S. G. Podkolzin, *J. Phys. Chem. B* **2005**, *109*, 2262 – 2274.
[27] B. Njegic, M. S. Gordon, *J. Chem. Phys.* **2008**, *129*, 124705.
[28] A. M. Joshi, W. N. Delgass, K. T. Thomson, *J. Phys. Chem. B* **2005**, *109*, 22392 – 22406.
[29] R. Todorovic, R. J. A. Meyer, *Catal. Today* **2011**, *160*, 242 – 248.
[30] R. G. Parr, W. Yang, *Density-functional theory of atoms and molecules*, Oxford University Press, Oxford, **1989**, pp. 127 – 133.
[31] D. Marx, J. Hutte in *Modern methods and algorithms of quantum chemistry, Vol. 1* (Ed.: J. Grotendorst), NIC Series, John von Neumann Institute for Computing, Jülich, **2000,** pp. 301 – 349..
[32] P. Giannozzi, F. de Angelis, R. J. Car, *J. Chem. Phys.* **2004**, *120*, 5903 – 5915.
[33] P. Giannozzi, S. Baroni, N. Bonini, M. Calandra, R. Car, C. Cavazzoni, D. Ceresoli, G. L. Chiarotti, M. Cococcioni, I. Dabo, A. Dal Corso, S. De Gironcoli, S. Fabris, G. Fratesi, R. Gebauer, U. Gerstmann, C. Gougoussis, A. Kokalj, M. Lazzeri, L. Martin-Samos, N. Marzari, F. Mauri, R. Mazzarello, S. Paolini, A. Pasquarello, L. Paulatto, C. Sbraccia, S. Scandolo, G. Sclauzero, A. P. Seitsonen, A. Smogunov, P. Umari, R. M. Wentzcovitch, *J. Phys. Condens. Matter* **2009**, *21*, 395502 – 395519.
[34] J. P. Perdew, K. Burke, M. Ernzerhof, *Phys. Rev. Lett.* **1996**, *77*, 3865 – 3868.
[35] N. Troullier, J. L. Martíns, *Phys. Rev. B* **1991**, *43*, 1993 – 2006.
[36] X. Gonze, P. Kackell, M. Scheffler, *Phys. Rev. B* **1990**, *41*, 12264 – 12267.
[37] H. J. Monkhorst, J. D. Pack, *Phys. Rev. B* **1976**, *13*, 5188 – 5192.
[38] *CRC Handbook of chemistry and physics*, (Ed.: D. R. Lide), FL, Boca Raton, **2000**, pp. 9 – 16.
[39] M. Elango, R. Parthasarathi, V. Sabramanian, C. N. Ramachandran, N. Sathyamurthy, *J. Phys. Chem. A* **2006**, *110*, 6294 – 6300.
[40] J. Koput, *J. Mol. Spectrosc.* **1986**, *115*, 438 – 441.
[41] C. Kittel, *Introduction to Solid State Physics*, 7edth edWiley, New York, **1986**, pp. 23 – 24.
[42] Gaussian 09, Revision A.1, M. J. Frisch, G. W. Trucks, H. B. Schlegel, G. E. Scuseria, M. A. Robb, J. R. Cheeseman, G. Scalmani, V. Barone, B. Mennucci, G. A. Petersson, H. Nakatsuji, M. Caricato, X. Li, H. P. Hratchian, A. F. Izmaylov, J. Bloino, G. Zheng, J. L. Sonnenberg, M. Hada, M. Ehara, K. Toyota, R. Fukuda, J. Hasegawa, M. Ishida, T. Nakajima, Y. Honda, O. Kitao, H. Nakai, T. Vreven, J. A. Montgomery, Jr., J. E. Peralta, F. Ogliaro, M. Bearpark, J. J. Heyd, E. Brothers, K. N. Kudin, V. N. Staroverov, R. Kobayashi, J. Normand, K. Raghavachari, A. Rendell, J. C. Burant, S. S. Iyengar, J. Tomasi, M. Cossi, N. Rega, J. M. Millam, M. Klene, J. E. Knox, J. B. Cross, V. Bakken, C. Adamo, J. Jaramillo, R. Gomperts, R. E. Stratmann, O. Yazyev, A. J. Austin, R. Cammi, C. Pomelli, J. W. Ochterski, R. L. Martin, K. Morokuma, V. G. Zakrzewski, G. A. Voth, P. Salvador, J. J. Dannenberg, S. Dapprich, A. D. Daniels, . Farkas, J. B. Foresman, J. V. Ortiz, J. Cioslowski, D. J. Fox, Gaussian, Inc., Wallingford CT, **2009**.

Received: July 21, 2014
Published online on September 26, 2014